TRENDS IN ANIMAL AND PLANT SCIENCES
https://doi.org/10.62324/TAPS/2025.064
www.trendsaps.com; editor@trendsaps.com
E-ISSN: 3006-0559; P-ISSN: 3006-0540

RESEARCH ARTICLE

Assessing the Effects of Climate Change on the Runoff of Glaciers and Snowmelt in a Mountainous Region using Remote Sensing and Snow Runoff Modeling: A Case Study of Gilgit Baltistan

Fiza Saleem

Centre for Integrated Mountain Research (CIMR), University of the Punjab Quaid E Azam Campus, Lahore, Pakistan
***Corresponding author:** fzs22064@gmail.com

Article History: 25-04 Received: 02-Dec-2024 Revised: 25-Feb-2025 Accepted: 27-Feb-2025

ABSTRACT

Although alpine glaciers are not directly affected by human populations, they are vulnerable to the repercussions of climate change resulting from human activity. The main origin of water in the Indus River is the process of snow and glacier melting in the northern part of Pakistan, which includes the majestic Himalayas, snow-covered Karakoram, and Hindukush mountains. Accurate measurement of the amount of water flowing in rivers due to the melting of snow can help in efficiently managing the necessary water resources required for generating hydropower and irrigation purposes. The main objective of this study was to evaluate the impact of climate change on the discharge of glacial meltwater in the Gilgit River basin. The Shuttle Radar Topographic Mission (SRTM) data is employed to generate the Digital Elevation Model (DEM) for the specified region. The SRM employs various elements like Snow Cover Depletion curves, temperature, and precipitation, as well as features such as degree-day factor, recession coefficient, runoff coefficients, time lag, critical temperature, and temperature lapse rate. However, snow cover numbers are both simple and essential for the SRM. The extent of the snow-covered region is determined by the utilization of satellite data acquired from the Moderate Resolution Imaging Spectroradiometer (MODIS).

The study findings indicate that the yearly precipitation varies between 148 mm and 700 mm, with an average basin precipitation of 350 mm. The average monthly flow of the basin is 288 cubic feet per second (cusec). The basin's water production is determined to be 9.09 billion cubic meters (750 millimeters). The initial snow in the Gilgit River basin contributes approximately 78.3% to the total runoff, whilst rainfall contributes 19.5%. The contribution of new snow to runoff is rather low, at around 2.2%. The average yearly temperature is projected to rise by approximately 0.30°C between 2011 and 2030, 1.30°C between 2031 and 2050, and 3.1°C between 2051 and 2099. The mean annual temperature of the Gilgit catchment is projected to rise by 4.7 °C by the end of the 21st century. By raising the yearly maximum and minimum temperature by 1.24°C, there will be a 16% rise in summer flows. Furthermore, if this temperature is further increased to 2.78°C, there will be a 34% increase in summer flows. An observation revealed that a 10% increase in the cryosphere area results in a 13% rise in summer flows, while a 20% increase in the cryosphere area leads to a 27% increase in summer flows in the Gilgit River.

Key words: Climate change, Remote sensing, Snow runoff modeling

INTRODUCTION

Pakistan is home to 5,218 glaciers, which make up 15,041 km2 of the Hindukush-Karakoram-Himalaya region. This region has a total of 54,000 glaciers (Bajracharya & Shrestha, 2011). The mountainous regions in northern Pakistan are blessed with a multitude of rivers that has significant potential for water resources and the generation of electricity (Ahmad et al., 2012). A significant number of these rivers remain untapped in terms of their potential as water resources. Exploring the potential of these rivers can enhance hydropower output and water supplies in these areas. Most of the water in the river Indus comes from snow and glaciers melting in the North of Pakistan, which includes lofty Himalayas, snow covered Karakoram and Hindukush mountains (Bookhagen and Burbank, 2010; Immerzeel et al., 2012 & 2013).

The transformation of snow and ice into water is called snowmelt, which needs the contribution of vitality (warm). The material science of dissolving snow and the change of soften water into spillover are essential segments of snow hydrology. Snowmelt is the general consequence of various warmth exchange mechanisms to the snowpack. The sun is a definitive wellspring of vitality in charge of the dissolving of snowpack. There is unpredictable cooperation between

Cite This Article as: Saleem F, 2025. Assessing the effects of climate change on the runoff of glaciers and snowmelt in a mountainous region using remote sensing and snow runoff modeling: a case study of Gilgit Baltistan. Trends in Animal and Plant Sciences 5: 29-45. https://doi.org/10.62324/TAPS/2025.064

the approaching sun-oriented radiation, the earth's environment, and the landscape surface. Consequently, several moderate strides during the time spent on vitality exchange to the snow surface must be examined to comprehend the procedure of snowmelt and furthermore to make quantitative estimations of the softening (Tanmoyee & Abdul 2015).

The glaciers in the Himalayan region are the largest in the world and are commonly referred to as the 'third pole'. The area encompasses the most elevated mountains on Earth, which includes all 14 summits surpassing an altitude of 8000 m. This region serves as the source of 10 major rivers, namely the Ganges, Indus, and Brahmaputra. These rivers are fed by the melting of snow and glaciers. The river basins in this area provide food and hydro-energy to over 3 billion people. Over the past century, this region has undergone numerous alterations in land use and land cover, encompassing climatic change as well. The alterations in climatic circumstances in this area directly impact the outflow of melted snow and the balance of mass in glaciers (Adam et al., 2009).

The MODIS instrument was launched by the Earth Observation System (EOS) on two platforms: Terra (EOS AM) on December 18, 1999 and Aqua (EOS PM) on May 4, 2002. The satellites' orbit around the Earth is synchronized in such a way that Terra crosses the equator from north to south in the morning, while Aqua crosses the equator from south to north in the afternoon. The MODIS snow cover data is transmitted globally in the form of 10-degree by 10-degree tiles at the equator. The entire globe is covered by a total of 36 horizontal (H) and 18 vertical (V) tiles, each with an area of 1200 km × 1200 km. NASA offers the MODIS 8-day composite maximum snow-cover product, which has a spatial resolution of 500m, for no charge (Baede et al., 2001).

The effect of environmental change in the Himalayas is higher on the earth of higher temperatures (Immerzeel et al., 2012). The vulnerability later on mountain water assets joined with the Indus bowl's substantial reliance on these upstream water assets, makes the Indus bowl an environmental change hotspot. This weakness is upgraded by a normal expansive territorial populace development in the coming decades, related with increments in water and vitality request in the bowl. Outrageous climate occasions are probably going to wind up more regular in the locale later on, which presents genuine dangers for a district which is now confronting extreme flooding occasions and other common risks. Any modification in the flow design in this waterway because of atmosphere prompted changes is probably going to influence the jobs of the populace. Investigations of glacierized bowls in various locales have been completed to enhance the comprehension of environmental change impacts on the bowl hydrology and on how water accessibility may be influenced by environmental change in this area. It is accordingly important to appraise the snowmelt spillover from this catchment. An examination by Bolch (2007) on icy mass withdraw in Tein Shan, Kazakhstan demonstrated that the icy mass withdraw was not homogenous but rather relied upon size, area and atmosphere administration. Just couple of concentrates as of now addresses the planning and advancement of ice sheets and related changes in spillover. A thorough investigation of reaction of glacierized bowls to environmental change in the Himalayas is as yet missing, essentially as a result of the blocked off landscape, absence of watched climatic information, and the way that reaction of icy masses isn't uniform all through the Himalayan.

Problem Statement

The water resources system is normally based on the presumption of stationary hydrological processes. According to recent studies and major flood events, the difference in hydro-meteorological changes is beyond the limits of stationary procedures. The anticipated global climate change is predicted to modify the patterns of precipitation and runoff, placing substantial strain on water supplies at both regional and global levels (Lightfoot & Ratzer, 2024). The diverse range of climatic phenomena impacts flood occurrences, leading to the occurrence of river floods, flash floods, urban floods, sewer floods, glacial lake outburst floods, and coastal floods. The intensity and frequency of floods and snowmelt runoff are significantly affected by increased precipitation as a consequence of climate change. This study aims to characterize the Gilgit watershed to get a deep insight into its work. Gilgit watershed is located in the north of Pakistan and remains snow-covered throughout the year. Water from snow melt adds to the Gilgit River as well as feeding adjacent croplands and domestic needs.

Pakistan's economy is heavily dependent on agriculture, which in turn relies on the Indus Basin Irrigation System (IBIS). The IBIS encompasses a geographical area of 22 million hectares (MHa), with irrigated land accounting for 85% of the overall food output in the country (Khan et al., 2024). The impact of climate change on water resources is a significant concern on a global scale (Farhan et al., 2024). Commonly mentioned hydrologic concerns include anticipated alterations in flow measurement, variability, and timing. The alterations can significantly affect the transboundary river basins, where there are notable differences in the economic, political, and social contexts of the countries involved.

The glacial meltwaters originating from the Karakoram glaciers have a significant influence on the water flow of the major Indus river. Therefore, any alterations in precipitation and temperature immediately impact the amount of water discharged into the river. Archer and Fowler (2004) and Fowler and Archer (2006) demonstrated a decline in river flows from the primary central Karakoram basins during the last 20 years. They propose that a significant portion of winter precipitation is being stored for an extended period due to glacial surges.

Quantitative analysis of climate change's hydrologic effects is crucial for comprehending and evaluating the potential water resource problems related to water supply, power generation, and agriculture. It is also vital for future water resource planning, reservoir design and management, and preservation of the natural environment.

Research Objectives

The main objective of this study was to analyze the impact of climate change on glacier and snowmelt runoff of Gilgit River basin. In order to meet the main objective of the study, the following specific research objectives were chosen:

1. To investigate the hydrological regime in area.
2. To stimulates the runoff in the Gilgit River basin.
3. To forecast the short term and seasonal runoff forecasts. To assess the possible climate change on water resources of Gilgit River basin.

MATERIALS AND METHODS

Study Area

Location

Gilgit basin was decided as the area of interest for this study due to several reasons. Most of the world glaciers lie in Gilgit, the reserves of freshwater are present over there in solid form i.e snow and ice (Fig. 1). It is due to all those glaciers and snow melt which add to Indus River and makes it mighty in its flow. More over Gilgit basin includes diversity of aspects such as huge mountains and definitely major rivers also have to pass through mountainous ranges. On the other hand the trend of industrial development, Road network up-gradation, Trade routes and several other aspects of urbanization are taking place in the basin. If any adverse effect of all such activities confronts in the natural phenomenon of Gilgit watershed the water quality, ecosystem balance and health of watershed will be affected. This delicate balance of nature needs to be maintained so to enhance importance of Gilgit basin, its characterization was taken up as research study, for perspective of its maintenance and management.

Drainage Network of Gilgit River Basin

The drainage network efficiently conveys water and sediment from a basin through a single exit, known as the maximum order of the basin. This outflow is typically the highest order stream inside the basin, and is termed the order of the basin. The size of rivers and basins varies significantly depending on the hierarchical structure of the basin. The first stage of basin analysis entails the organization of watercourses. Studying the parameters of stream networks is crucial for analyzing basin characteristics (Liang et al., 2002). The streams have been ranked using the methodology described by Strahler (1964). The stream order was observed up to 6. The stream numbers corresponding to each stream order are provided in Table 1. A total of 313 streams were detected, with 231 classified as first order, 56 as second order, 18 as third order, 5 as fourth order, 2 as second order, and 1 as an indication in sixth order. First-order streams have the highest stream count. Furthermore, Fig. 2 demonstrates a decline in the total count of stream segments as the stream order increases. The drainage patterns of the stream network inside the basin predominantly display a dendritic type, indicating a consistent texture and lack of structural impact, as illustrated in Fig. 2.

Table 1: Stream order, stream number, mean stream length and stream length ratio of Gilgit River Basin.

Stream Order, U	Stream Numbers, N_U	Stream Length, L_U (Km)	Mean Stream Length, L_{sm} (Km)	Stream Length Ratio, RL	Bifurcation Ratio, R_b
1	231	1182.42	5.12	0.46	-----
2	56	541.75	9.67	0.43	4.13
3	18	231.86	12.88	0.41	3.11
4	5	94.55	18.91	1.24	3.60
5	2	117.34	58.67	0.68	2.50
6	1	79.97	79.97	-----	2.00
Total	313	2247.89	-----	-----	-----
Mean	-----	-----	7.18	0.64	3.07

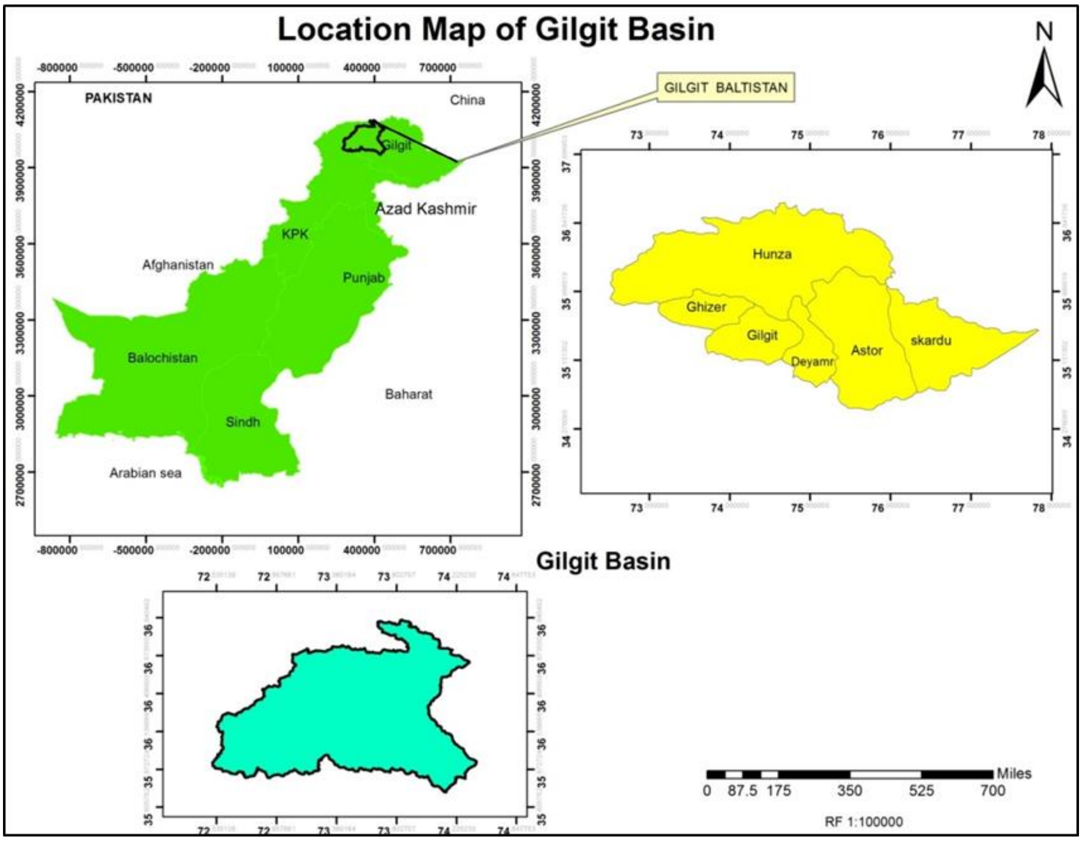

Fig. 1: Location of study area.

Longest Flow Path (L_b)

The length, as described by Schumm (1956), refers to the longest dimension of the basin that runs parallel to the major drainage line. In their 1973 study, Gregory and Walling defined length as the maximum distance within a basin, with one end being the mouth. The length of the flow path is 239.96 kilometers.

Basin Perimeter (P)

The basin perimeter refers to the outer edge of the watershed, which encompasses its entire area. It is quantified along the boundaries of watersheds and can serve as a gauge for the dimensions and configuration of a watershed. The basin has a perimeter of 964.17 kilometers.

Basin Area

The extent of the watershed is a significant metric, similar in importance to the length of the stream drainage. Schumm (1956) discovered a compelling correlation between the overall size of a watershed and the total length of its streams, which is influenced by the areas that contribute to it. Runoff volume rates are proportional to the size of the watershed. To ensure that erosion control structures and channels are designed to handle maximum runoff, it is vital to calculate the peak runoff rate. The type of basin with respect to basin is categorized into watershed (area up 1,000 Km^2), sub-catchment (1,000-7,000 Km^2), catchment (7,000-30,000 Km^2) and basin (30,000-95,000 Km^2). This drainage basin has an area of 12703 Km^2 and according to above mentioned criteria basin fall into catchment.

Topography

According to Fig. 3, the Gilgit basin is located between 1418 and 7060 meters above mean sea level (AMSL). Among the many climatic characteristics, including temperature and snowfall, elevation is a crucial one (Zhang et al., 2008). Snowmelt and snow accumulation processes in mountainous watersheds are strongly influenced by elevation changes (Pomeroy and Burn, 2001).

Hypsometric Analysis (Hs)

The area elevation curve is derived by graphing the elevation of the contour against the area or percentage of area, either above or below that elevation, as seen in Fig. 4. The area elevation curve is alternatively referred to as the hypsometric curve for the basin. The median elevation refers to the elevation that corresponds to the midpoint of the catchment area, and it is calculated based on the area-elevation curve. The median elevation, representing the value at the center of the data set, is determined to be 4100 m for 50% of the total area. On the other hand, the mean elevation, which is the average value, is calculated to be 4052.73 m.

Data Base

The collection of following data was considered in order to analyze the climate change and its impacts on the streamflows in Gilgit basin (Table 2).

Meteorological Data

In order to conduct this study, the Pakistan Meteorological Department (PMD) and WAPDA provided available daily meteorological time series data from eight different stations. The stations' average monthly precipitation (P), maximum and minimum temperatures (Tmax and Tmin), and site-specific information are displayed in Table 3.

Table 2: Type of data used in the present study and their source.

Data Type	Source	Resolution/Scale	Description/Period of Record
Topography	USGS National Elevation Dataset	90 × 90 m	DEM (Elevation)
Landuse data	European Space Agency (ESA) Global Land Cover http://ionia1.esrin.esa.int/	300 × 300 m	Classified land use such as forest, agriculture, crops, water etc.
Soil data	FAO– International Soil Reference and Information Centre (ISRIC)	1 km	Classified soil and physical properties as sand silt clay bulk density etc.
Climatic data	Pakistan Metrological Department (PMD), Water and Power Development Authority (WAPDA)	Daily	Precipitation, Temperature, Solar radiation, Wind Speed (1961-2010)
Hydrological data	Water and Power Development Authority (WAPDA)	Daily	Streamflows (1961-2010)
MODIS)		Daily	2001-2010

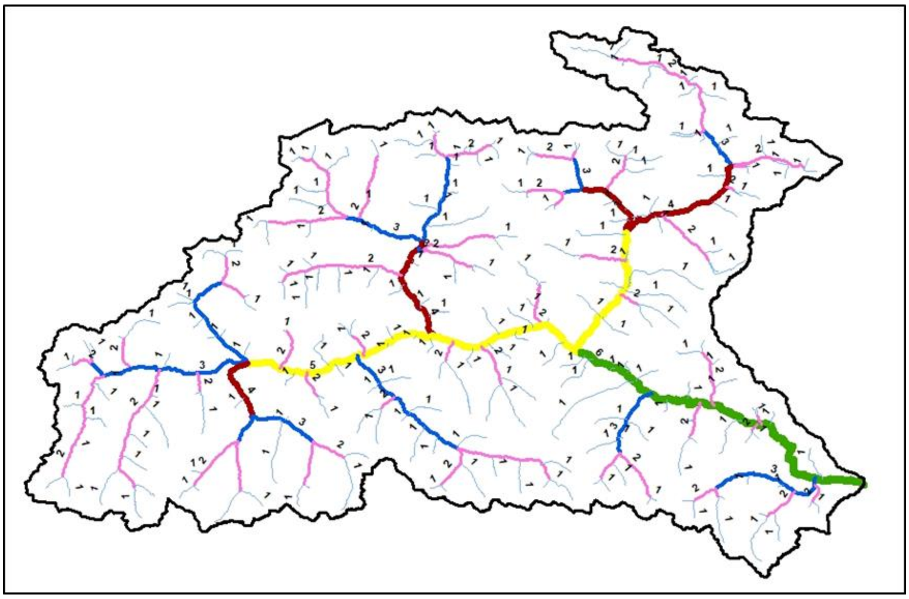

Fig. 2: Stream order of Gilgit Basin.

Table 3: List of climatic stations used in present study and their characteristics.

Sr. No.	Climatic Station	Latitude (dd)	Longitude (dd)	Elevation (m)	Area (Km²)	Prec. (mm)	Max. Temp (°C)	Min. Temp (°C)	Weight of Station Area of Basin (in fraction)	% Area of Basin (%)
1	Gilgit	35.9	74.3	1460	531.7	148	23.9	7.6	0.042	4.19
2	Gupis	36.2	73.4	2156	1697	227	18.8	6.6	0.134	13.36
3	Khot Pass	36.5	72.6	3505	212.6	485	7.1	-4	0.017	1.67
4	Naltar	36.1	73.2	2100	2138.7	701	11.1	2	0.168	16.84
5	Shendure	36.1	72.5	3719	1552.6	192	5.7	-4	0.122	12.22
6	Ushkore	36	73.4	3353	1836.7	335	10.3	1.6	0.145	14.46
7	Yasin	36.4	73.3	3353	3395.5	322	9	0.8	0.267	26.73
8	Ziarat	36.9	74.3	3688	1338	274	7.7	-2.1	0.105	10.53

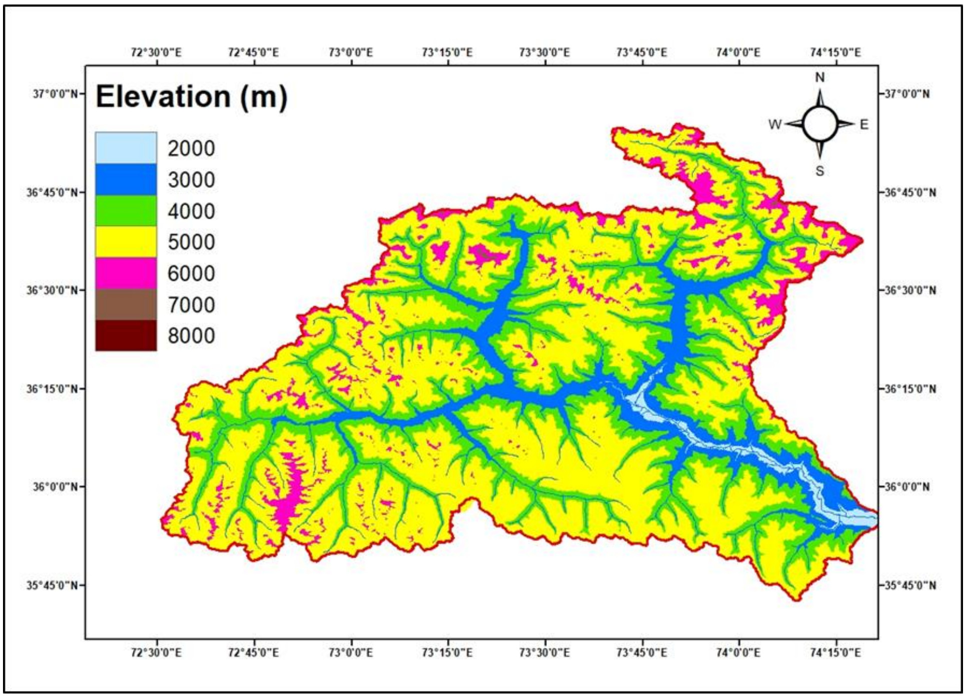

Fig. 3: Topography of Gilgit River Basin.

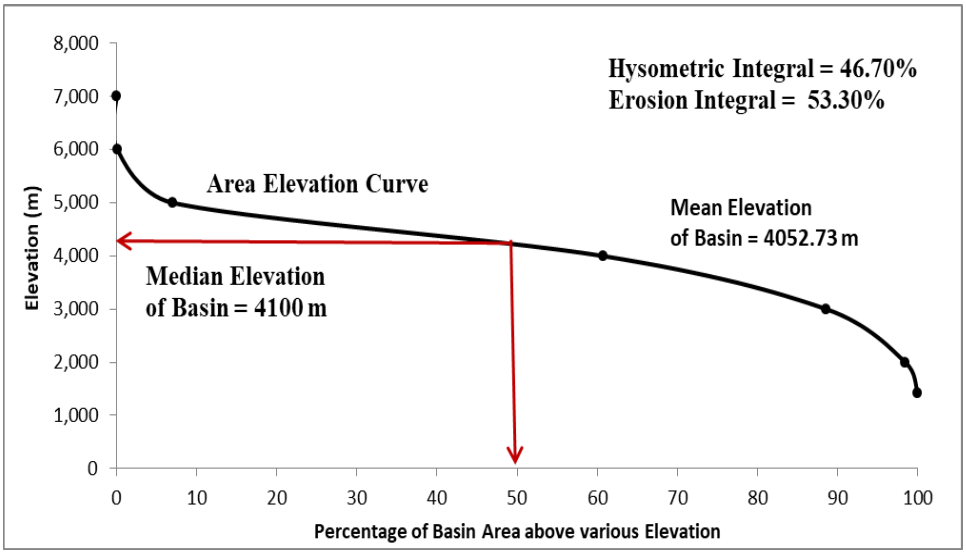

Fig. 4: Area elevation curve (hypsometric curve) of Gilgit River basin.

Climatic Characteristics of Gilgit Basin

Temperature Analysis

For this study eight climatic stations were selected their characteristics with site information are given in Table 3. The monthly average maximum, minimum, and mean temperatures for each year were calculated based on the daily maximum, daily minimum, and daily mean temperatures. The mean daily temperatures are calculated by taking the average of the highest and lowest temperatures recorded each day.

Maximum Temperature

The mean monthly temperature of each station is plotted in Fig. 5. The means of maximum temperature T_{max} vary from -8.8 °C to 36.13 °C. The high-elevated stations show the lowest temperatures whereas low-elevated stations show the highest temperatures. Spatial distribution and isotherm of annual maximum temperature is shown in Fig. 6. This Figure depicts that western side has lower temperature while the eastern side has the higher. The highest temperature was

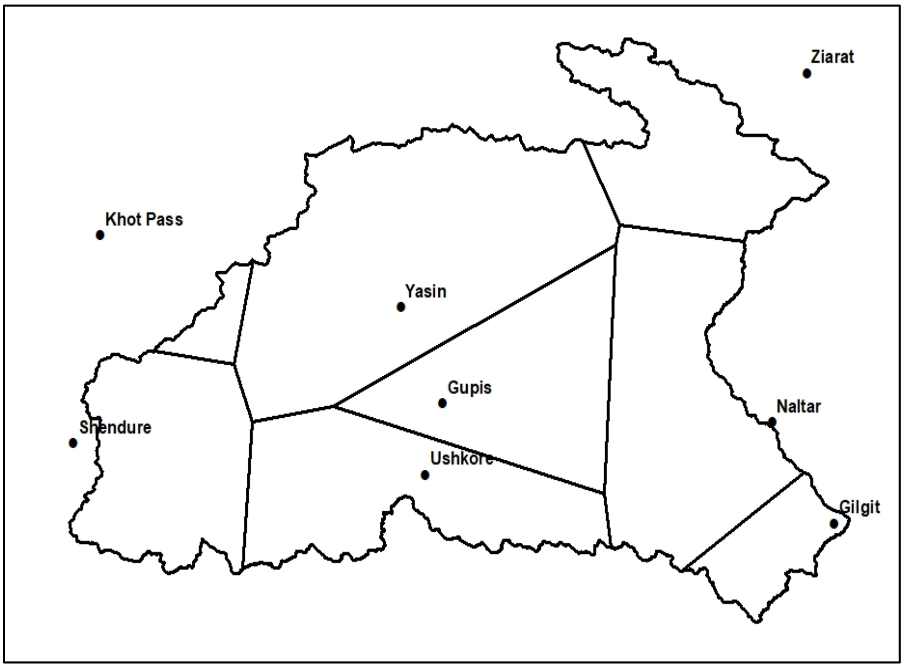

Fig. 5: Thiessen Polygon in Gilgit basin

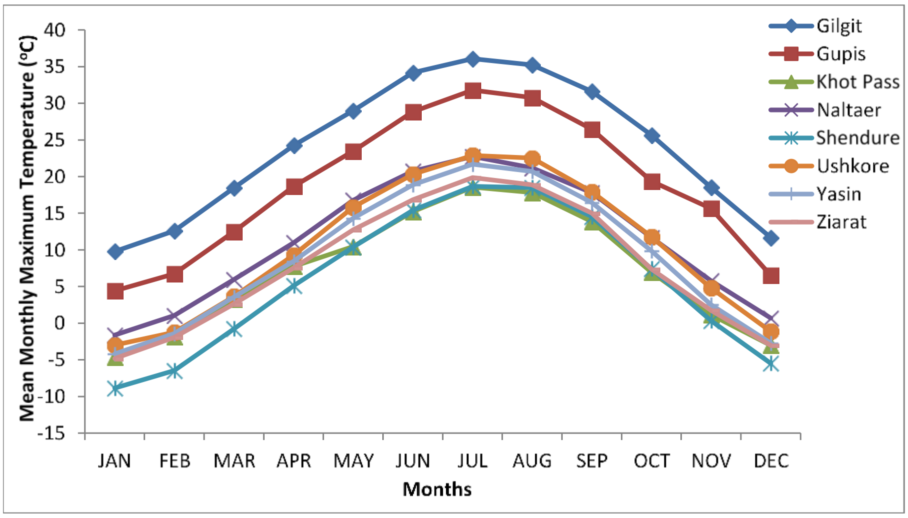

Fig. 6: Mean monthly distribution of maximum temperature in climatic stations of Gilgit basin.

Table 4: Calibration Parameter values used in SRM

Parameter	Parameter Values
Temperature Lapse Rate (°C/100m)	0.64
Tcrit (°C)	0
Degree day factor (cm °C^{-1} d^{-1})	0.3-0.75
Lag time (hrs)	18 hrs
Runoff coefficient for snow	0.03-0.45
Runoff coefficient for rain	0.05-0.48
Rainfall contributing area	RCA=0 -1
Reference elevation	3060 m
Initial Discharge	85.47cumec
Rainfall threshold	6.0 cm
Recession coefficients	Xcoeff. =1.08-1.09 and Ycoeff. = 0.02

Table 5: Statistical ananlysis of SRM validation

Statistical parameter	**Year 2005**	**Year 2006**
Volume Difference, Dv	-2.46	-1.43
Coefficient of model Efficiency %	0.95	0.911
Coefficient of determination %	0.96	0.912
Pearson correlation coefficient %	0.984	0.95
Standard Error (cumec)	170.66	93.18
Root mean square error (cumec)	737.53	288.13
Mean absolute error (cumec)	12.60	4.27
No. of observation	365	365

in the month of June and lowest in January. Mean annual and seasonal distribution of maximum temperature for the basin is shown in Fig. 7. The summer season has highest temperature (22.2 °C) while the winter has lowest (-1.0 °C).

Minimum Temperature

Mean monthly minimum temperature of each station is plotted in Fig. 9. Means of minimum temperature T_{min} vary from -16.6 °C to 18.1 °C. The high elevated stations. This Figure depicts that western side has lower temperature while the eastern side has the higher. The overall mean basin minimum temperature is 1.2 °C and varies from -8.3 °C to 12.2 °C as shown in Fig. 8. The highest temperature was in the month of June and lowest in December. Mean annual and seasonal distribution of minimum temperature for the basin. The summer season has highest temperature (11.1 °C) while the winter has lowest (-9.0 °C).

Precipitation Analysis

Mean monthly precipitation varies from 9 mm (Gilgit) up to 110 mm (Naltar) and indicate large spatial variation. Mean annual precipitation ranges from around 148 mm (Gilgit) to 700 mm (Naltar) that has highest elevation.

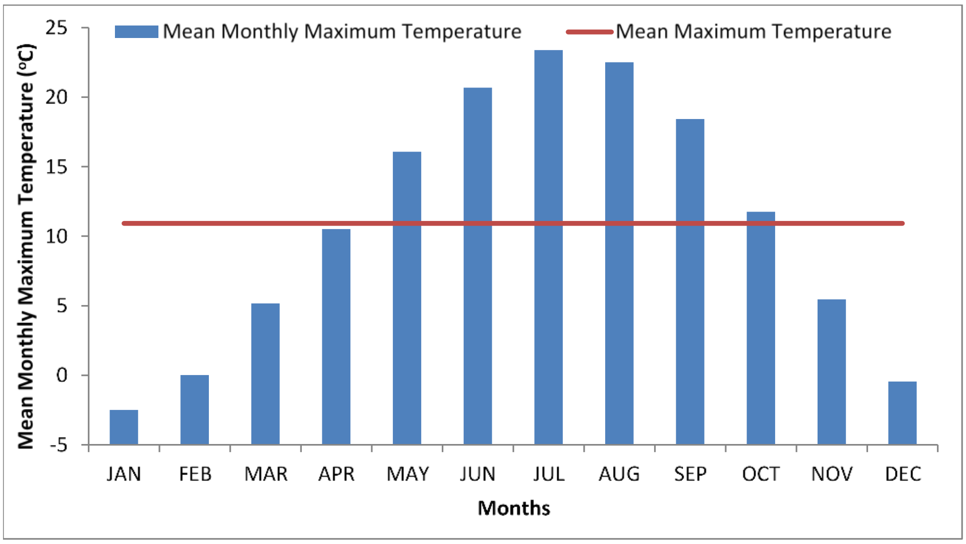

Fig. 7: Mean monthly distribution of maximum temperature for Gilgit basin.

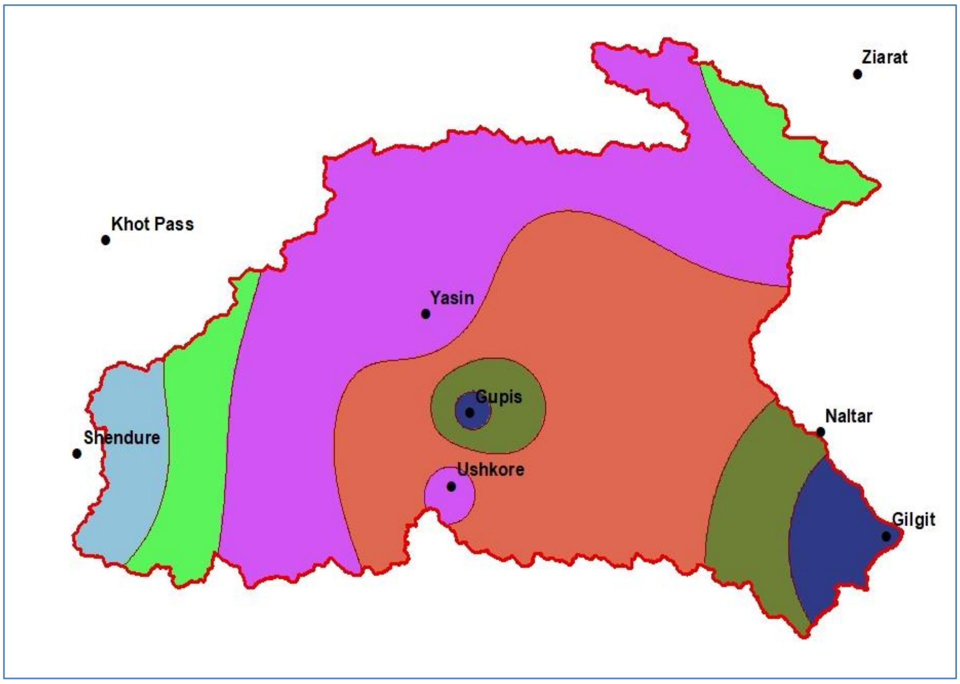

Fig. 8: Spatial distribution and isotherm of annual minimum temperature in Gilgit basin.

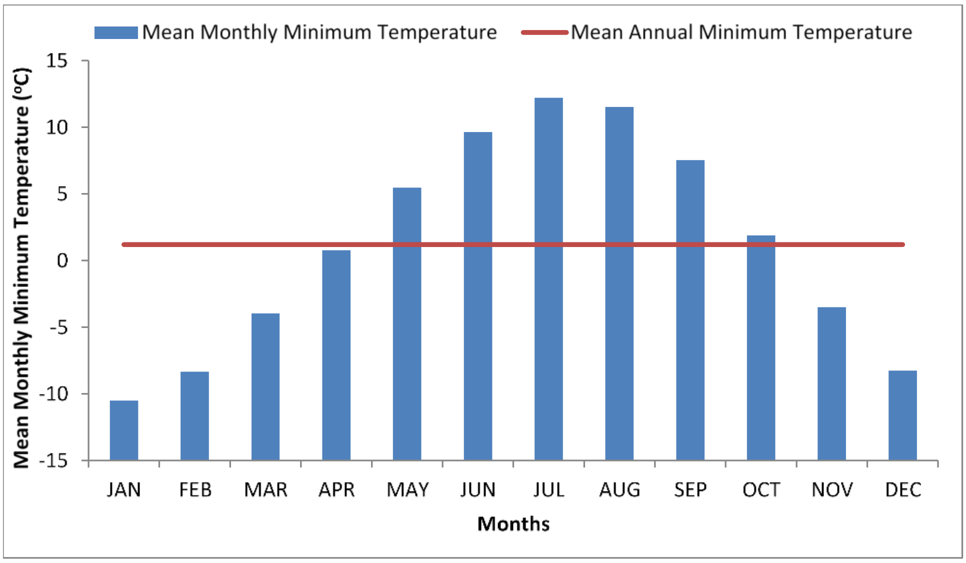

Fig. 9: Mean monthly distribution of minimum temperature for Gilgit basin.

Hydrological Characteristics of Gilgit Basin

The highest mean monthly flow appears in the month of July with a value of 908 cumec and minimum in the month of March with a value of 50 cumec while the mean monthly flow is 288 cusec. The summer season has the major contribution of flows which is about 67% of total annual flows. The trends and temporal distribution of the annual mean, minimum and maximum streamflows is given in Fig. 12 and 13 respectively. This analysis of trend indicate that mean and maximum flows have increasing trend while the low flows have decreasing trend. Highest flow was observed in 2013 with the value of 1721 cumec.

Table 6: Contribution of Snow and Rain to the Total Runoff of Gilgit River

Colour	Source	Contribution to total Runoff (%)
Red	Snow + Glacier melt	78.3
Green	New Snow	2.2
Blue	Rain	19.5
	Total	100

Table 7: Impact of Decrease in Average Annual 'T' on Flows

Scenario	Tavg.(C°) Fall	Decrease in Summer Flow (%)
1st	T-1	3
2nd	T-2	7

Table 8: Trend of Maximum Temperature (2011-2099)

	Maximum Temperature (°C)		
Period/Season	Annual	Winter	Summer
2011-2030	0.88	0.23	1.31
2031-2050	1.57	1.46	1.54
2051-2099	2.67	4.78	0.85

Table 9: Trend of Minimum Temperature (2011-2099)

	Minimum Temperature (°C)		
Period/Season	Annual	Winter	Summer
2011-2030	0.48	0.91	0.66
2031-2050	0.91	0.79	1.19
2051-2099	2.89	6.40	0.10

Table 10: Percentage Flow rise due to Max. And Min. T (°C)

Period/Season	Annual Max/Min 'T' Rise (°C)	Annual Flow (%)	Winter Flow (%)	Summer Flow (%)
2011-2030	0.68	6	2	7
2031-2050	1.24	15	4	16
2051-2099	2.78	33	8	34

Table 11: Percentage Flow Increase due to Winter Max. And Min. T (°C)

Period/Season	Winter Max/Min 'T' Rise (°C)	Winter Flow (%)
2011-2030	0.57	2
2031-2050	1.13	3.5
2051-2099	5.59	14

Table 12: Percentage Flow rise due to Summer Max. And Min. T (°C)

Period/Season	Summer Max/Min 'T' Rise (°C)	Summer Flow (%)
2011-2030	0.98	12
2031-2050	1.36	16
2051-2099	0.48	No significant change

MODIS Data

The data products are derived from radiometric measurements collected by the MODIS sensor installed on NASA's Terra satellite. The algorithms for both Spectral Clear-Sky Albedo (SCA) and Land Surface Temperature (LST) depend on the existence of "clear sky conditions." Therefore, in order to determine the condition of the snow cover or calculate its Land Surface Temperature (LST), it is crucial that the pixel in issue is free from clouds. Hence, the data used in this research are obtained from consecutive 8-day temporal aggregates that incorporate all the available observations throughout the defined period. Most satellite views in the Upper Indus region show partial cloud covering due to the cloud climatology. Generally, pixels located in valley bottoms see lower occurrences of cloud cover in comparison to pixels positioned on mountain summits. Consequently, the quantity of observations that contribute to 8-day aggregates will frequently be more in low elevation zones as opposed to higher ones.

The study employs MODIS snow products from both MODIS Terra and MODIS Aqua versions as the primary data source. The bias towards Terra is due to the reliance on the utilization of near-infrared data at 1.6 µm for the snow detection method (Sirguey, et al. 2009). Snow can be detected primarily by its characteristic of having a high level of visible reflection and a low level of reflectance in the near infrared, namely in MODIS band 6. The MODIS dataset comprises 315 bands, each offering daily and monthly statistics on snow cover for the year 2010. Each pixel has dimensions of 500 meters by 500 meters. The climate data comprises daily recordings of precipitation and temperature. This data is used to determine the association between the snow cover change pattern and the local climate change. Due to the significant difference in size between the snow cover data and the climatic data source, only data from the same day are used in the subsequent study.

Methodology

Gilgit Watershed Delineation

Gilgit watershed was delineated from SRTM Digital Elevation Model (DEM).The resolution of SRTM DEM was 90m. DEM was processed in Arc View GIS. Following steps were involved in it:

a. Fill Sink
b. Flow Direction
c. Flow Accumulation
d. Stream Definition
e. Stream Segmentation
f. Catchment grid Delineation
g. Catchment Polygon Processing
h. Drainage line Processing
i. Adjoining Catchment Processing
j. Drainage Point Processing
k. Point Delineation

The Gilgit watershed delineated from DEM. The catchment area of Gilgit calculated is about 12671km^2.

Reclassification of DEM

The Gilgit DEM was classified into different elevation zones using Reclassify command from 3D-analyst Tool. The steps involved in Arc GIS are given below:

1. The Gilgit DEM was loaded into Arc GIS.
2. Reclassify command was used from 3D analyst tool to make different elevation classes of DEM.
3. The DEM was classified into six elevation zones.

The DEM was classified according to elevation range. The zone A is of low elevation (1415-2620m) and zone F is of high elevation (4897-7104m). Mean hypsometric elevation ($\bar{h}$) of Gilgit catchment was determined using Arc GIS and Erdas Imagine. The average hypsometric elevation for each zone was calculated. The base station temperatures are extrapolated to a specific height in order to calculate zonal degree-days. The most of the area of Gilgit watershed that is about 6792km^2 or 53.6% lies between elevation ranges of 3931 to 4897m. About seven to eight percent area of catchment is above 5000m elevation.

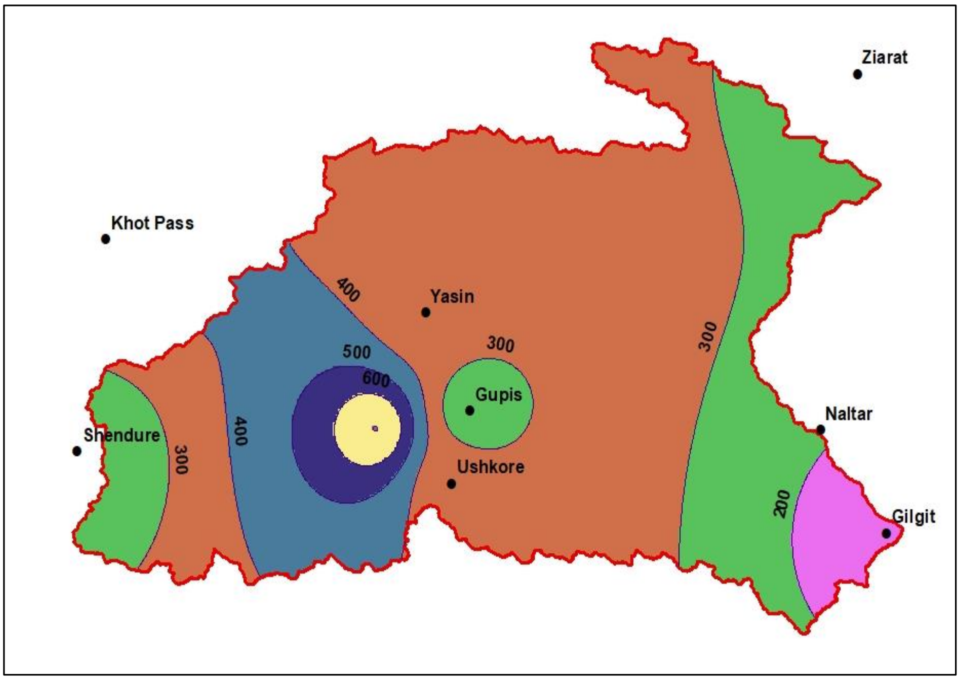

Fig. 10: Spatial distribution and isohyet of annual precipitation in Gilgit basin.

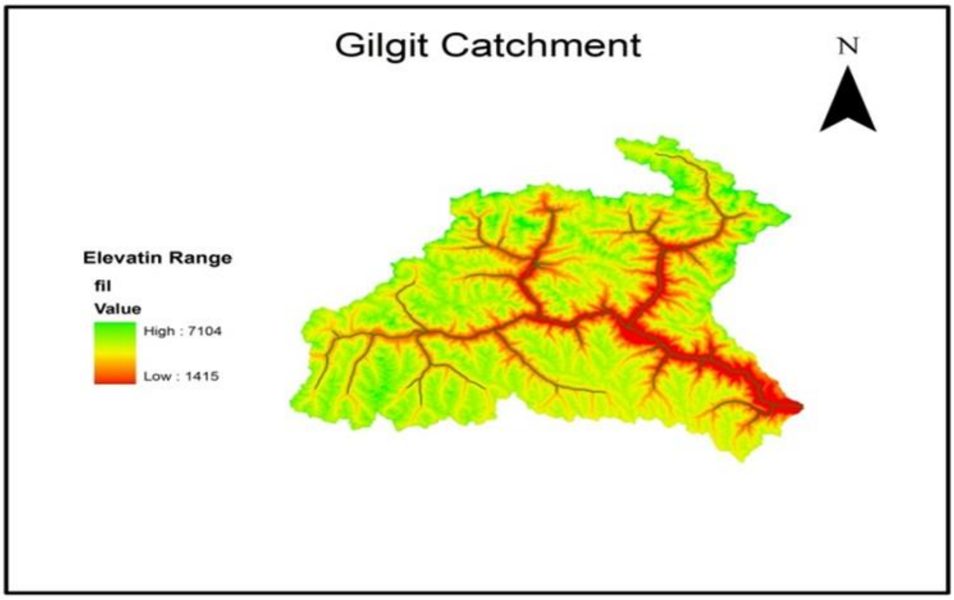

Fig. 11: Map of Gilgit watershed

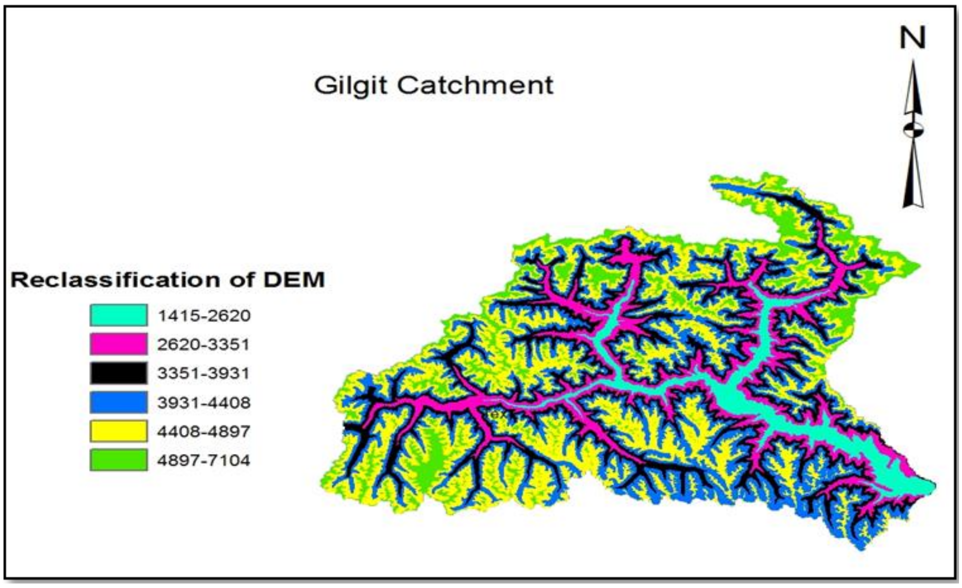

Fig. 12: Reclassified DEM

(i) Moderate Resolution Imaging Spectroradiometer (MODIS) Terra Data

The MODIS Terra product MOD10A1 was obtained from the National Snow and Ice Data Center (NSIDC). The data was downloaded daily. The website link is http://nsidc.org/data/modis/order_data.html. The snow cover data spanning a decade (from 2001 to 2010) was obtained for download. The MODIS10A1 product has a resolution of 500×500 meters.

MODIS Snow Cover Data Treatment

The MODIS data, initially stored in the Hierarchical Data Format – Earth Observing System (HDF-EOS), was transformed into the GEO-TIFF format to enable its utilization in Geographic Information Systems (GIS) applications. GIS is unable to accurately process HDF-EOS format, hence conversion to GEO-TIFF is required. The data was transformed into GEO-TIFF format using the HEG-Tool software.

HDF-EOS TO GEO-TIFF (HEG) Conversion Tool

The HDF-EOS to Geo-TIFF format can be easily converted using this utility. Its original intent was to enable users to reformat, re-project, stitch, mosaic, and sub-set HDF-EOS objects. The result file, Geo-TIFF, can be easily imported into popular GIS programs. Currently, HEG is compatible with HDF-EOS data sets from AMSR, AIRS, MODIS (AQUA and TERRA), MISR, and ASTER. You may find the download link for the HEG Tool below:
http://newsroom.gsfc.nasa.gov/sdptoolkit/HEG/HEGDownload.ht

Estimation of Snow Covered Area

The daily MODIS product (MOD10A1) was processed in Arc View GIS. The step wise procedure is given below:
1. Reclassified DEM of Gilgit catchment was loaded in Arc View GIS.
2. The daily MODIS tile in GEO-TIFF format was loaded and overlapped on Reclassified DEM in Arc View GIS.

Extract by Mask

The snow covered area that was overlapped over reclassified DEM was extracted using extract by mask command from special analyst tool of Arc view GIS.

MODIS tile was used as input raster and reclassified DEM was used as input raster or feature mask data. MODIS tile extracted consist of various variables such as snow covered area, clouds, non-snow covered area etc.

Extract by Attributes

To separate snow from other variables such as clouds and non-snow covered area extract by attributes command was used from spatial analyst tool.

The MODIS tiles in which snow counts percentage were more than 70% as compared to the clouds were used for further analysis.

The MODIS tile consists of various variables such as snow covered area, non- snow covered area, clouds cover, inland water etc. In attribute table, these variables are denoted by certain integer values such as 200 for snow and 50 used for cloud cover.

Zonal Statistics as Table

The snow counts obtained were further processed in Arc view GIS. The zonal statistics as table command was used to distribute snow counts into different elevation zones.

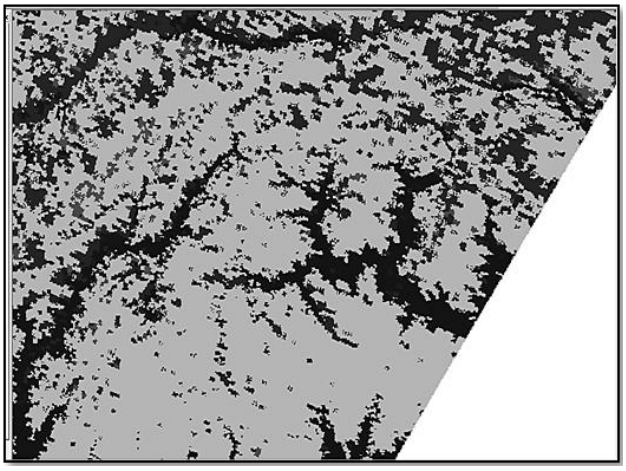

Fig. 13: Overlapping of MODIS tile over Reclassified DEM

Calculation of Snow Covered Area

The number of snow counts obtained from GIS were entered in excel sheet and multiplied it with a factor {(500m*500m/1000000) =0.25} and in this equation (500m*500m) is area of one snow count and then divided by (1000000) to convert snow covered area into square kilometer. The area of one snow count was multiplied by the total number of counts to get the total snow covered area in each zone. The (Conventional Depletion Curve) CDC values were calculated dividing snow covered area by zone area. The CDC value was used as input in SRM.

SNOWMELT-RUNOFF MODEL (SRM) Simulation Procedure

The Snowmelt-Runoff Model (SRM) is a hydrologic model that employs a conceptual, deterministic, distributed, and physically based methodology to simulate and forecast daily streamflow in mountain basins where snowmelt significantly contributes to the runoff. Recently, it has also been used to assess the impact of climate change on seasonal snow cover and runoff. The tiny Reservoir Model (SRM) was formulated by (Rango & Martinec, 2008) specifically for application in tiny basins located in Europe. The advancement of satellite remote sensing technology has facilitated the use of SRM to increasingly wider basins. The runoff calculations performed by SRM seem to be readily comprehensible. So far, the model has been utilized by numerous agencies, institutes, and universities in more than 100 basins, located in 29 distinct countries.

- Choosing a hydrological model.
- Utilize the ERDAS Imagine/Arc GIS program to demarcate the extent of snow coverage in satellite pictures.
- Watershed delineation performed using ArcGIS software.
- Partition the watershed into distinct elevation zones at regular intervals and plot the area elevation curve.
- Calculate the hypsometric elevation and snow cover extent for each elevation zone.

The weather data refers to the information and measurements collected about atmospheric conditions such as temperature, humidity, precipitation, wind speed, and atmospheric pressure.

- Create a graph illustrating the rate at which snow is diminishing in each zone over time.

Utilize the SRM 1.11 (snowmelt runoff model) to simulate the flow of water and determine the effects of climate change on stream flows. The flowchart illustrating the simulation of runoff using the Snowmelt Runoff Model can be shown in Fig. 14.

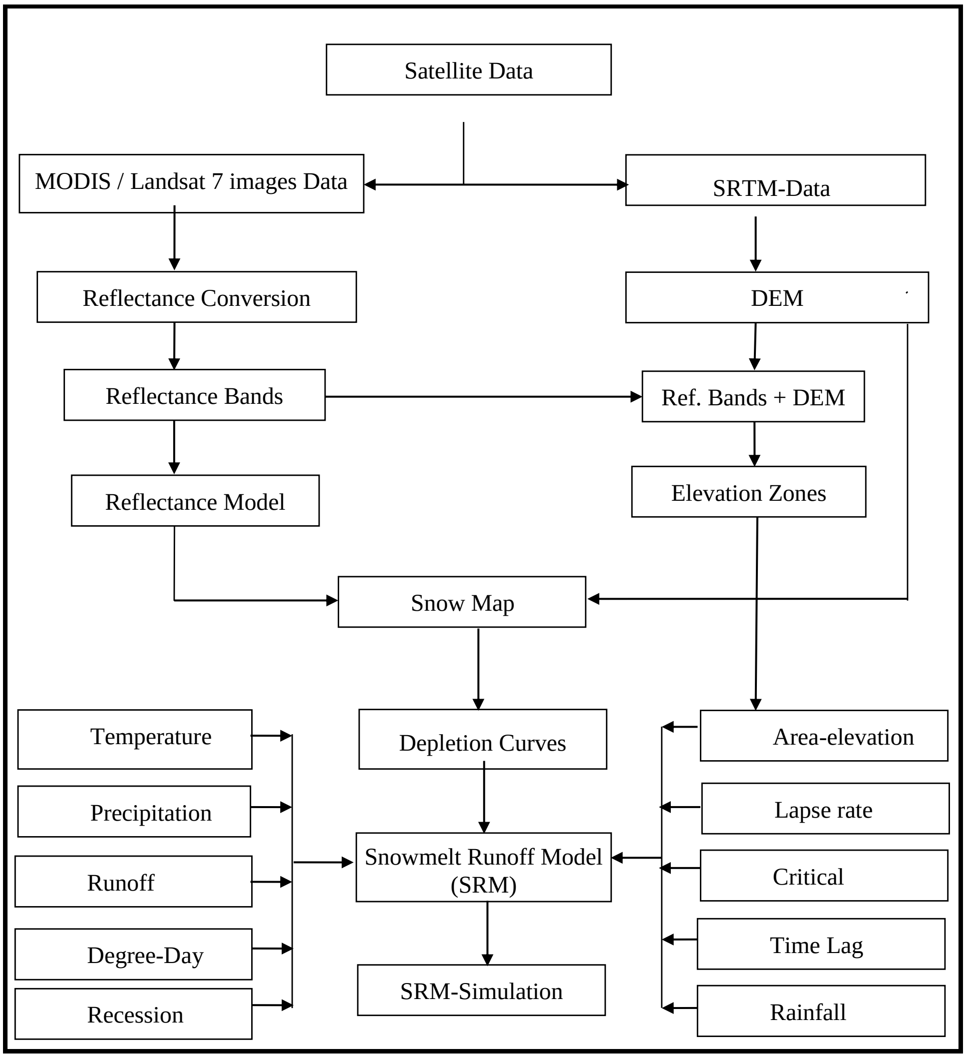

Fig. 14: Flowchart for runoff-simulation using Snowmelt Runoff Model.

• Calibration of the model.
• Calculate the impact of snowmelt and rainfall on stream flow at different time intervals and geographical locations.

Model Structure

Every day, the water resulting from the melting of snow and the precipitation is calculated, overlaid on the determined decrease in flow, and converted into daily discharge from the basin using the Equation:

$$Q_{n+1} = [C_{sn} \cdot a_n (T_n + \Delta T_n) S_n + C_{Rn} P_n] \frac{A.10000}{86400} (1 - K_{n+1}) + Q_n K_{n+1}$$

Basin Characteristics

Basin and Zone Areas

The parameters of SRM, such as basin area and elevation zone, are unique properties of a certain basin. Basin regions and elevation zones can be determined by using a topographic map of any size or by leveraging computer analysis, as long as a Digital Elevation Model (DEM) for the research basin is available.

Area-elevation Curve

The area-elevation curve is used in SRM to determine the zonal mean hypsometric height, which is then used as the reference elevation for extrapolating base station temperatures to calculate zonal degree days. The area-elevation curve and zonal mean hypsometric elevation can be derived from a Digital Elevation Model (DEM) using spatial analytic capabilities provided by a Geographical Information System (GIS). The computation of the regions enclosed by various elevation contours can be achieved using planimetering, a method that utilizes the boundaries of the zones and specific contour lines within the basin. The provided data can be graphed, specifically plotting the area against the elevation, and then an area curve can be produced. The automatic derivation of this area elevation curve is possible when the user has access to digital elevation data and computer techniques employed in an image processing system.

Model Variables

Temperature and Number of Degree-day

In SRM, the degree-day value is represented as a temperature. Temperature serves as a comprehensive metric for estimating the process of snowmelt. Additionally, temperature is a regular meteorological measurement that is readily obtainable, may be extended beyond the observed range, and can be predicted. To calculate the daily depth of snowmelt, the average degree-day value is computed for each zone.

Precipitation

During the snowmelt season, precipitation typically manifests as either rain or snow. In the field of meteorology, a crucial threshold known as the critical temperature is utilized to determine whether a given weather event will manifest as rain or snow. Precipitation is classified as rain when the temperature exceeds the crucial temperature, and as snow when it does not. The critical temperature is typically chosen to be slightly higher than the freezing point, however this can differ between different basins. The differentiation between rain and snow is significant in SRM due to the fact that the runoff from rain occurs concurrently with the rainfall, whereas the runoff from snow is typically delayed.

Snow-covered Area

A characteristic common to mountain basins is the steady reduction in the area covered by snow as the season for snowmelt advances. Snow covering is a crucial input variable for SRM. Daily snow coverage values can be derived from depletion curves, which can be created using periodic snow cover mapping.

Parameters of the Model

The Coefficient of Runoff

The SRM allows for distinct estimates of the runoff coefficient for snow and rain, as the runoff coefficient typically varies between snowmelt and rainfall. It is necessary to alter the runoff coefficient during the early phase of model simulation, particularly when the runoff simulation is not immediately effective.

Degree-day Factor

The degree-day factor in SRM is a crucial metric used to calculate the depth of water in snowmelt.

The degree-day factor, which varies with the seasons, was chosen within the range of 0.3 – 0.75 cm °C-1d-1 based on prior research conducted in Himalayan river basins (Dhami et al., 2018).

The Temperature Lapse Rate

The temperature lapse rate is a crucial element that greatly affects SRM models when used for temperature extrapolation. If temperature stations at various elevations are accessible, the temperature lapse rate can be predetermined using previous data. Alternatively, a suitable value must be determined by comparing data from nearby stations or considering the meteorological data source. The SRM simulations typically utilized a lapse rate of 0.65°C per 100 m (Rango & Martinec, 2008).

Critical Temperature

The crucial temperature is a mean temperature utilized in SRM to ascertain whether precipitation manifests as rain or snow. The critical temperature typically exceeds the freezing point and gradually decreases to approach 0°C as the snowmelt season advances.

Rainfall Contributing Area

Rainfall contributing area is a parameter used in SRM to determine whether rainfall runoff is included only from areas without snow (option 0) or from the entire basin or zone region (option 1). When option 0 is chosen in the SRM simulation, rainfall-runoff is only included in the snowmelt runoff in regions where there is no snow. Alternatively, selecting option 1 involves combining the runoff from rainfall with the runoff from snowmelt across the entire basin or zone region. The model simulation picks and sets many options in half-month intervals to identify the area that contributes to the overall rainfall. This is accomplished by considering the different phases of the snowmelt period.

Recession Coefficient

The recession coefficient is a vital model parameter as it signifies the proportion (1–k) of the daily melt-water from snow that adds to the daily runoff. The recession coefficient can be obtained by examining past discharge data through the equation formulated by (Rango & Martinec, 2008).

Time Lag, L

The diurnal variations in snowmelt runoff allow for the direct determination of the time delay based on the hydrographs from previous years.

Critical Temperature, TCRIT

The crucial temperature is the determining factor in distinguishing whether the observed or predicted precipitation will manifest as rain or snow. The accurate representation of this parameter is crucial for models that predict the formation and melting of the snow cover, as it significantly impacts the calculation of runoff. This influence is especially pronounced during the period of snow accumulation. SRM requires the critical temperature just to determine if precipitation directly results in runoff (rain) or, if the temperature is below the critical threshold, whether snowfall occurred.

Assessment of the Model Accuracy

The SRM computer application includes a graphical depiction of the computed hydrograph and the observed runoff. SRM utilizes two well-established accuracy metrics: the coefficient of determination, R2, and the volume difference, Dv. These criteria offer a more impartial assessment of the simulation's quality.

RESULTS & DISCUSSION

Snow Depletion Curves of Gilgit Catchment

Snow depletion curves illustrate the rate at which snow diminishes in various months and elevation zones. The snow depletion curves were generated by the utilization of Remote Sensing and Geographic Information Systems (GIS). The Conventional Depletion Curve (CDC) depicts the proportion of the snow-covered area in each elevation zone; the CDC value from each month was taken and then drew the graphs. The average snow-covered area in Gilgit varies from 10 % in summer to 85 % in winter. To check the variability of snow in different months, snow depletion curve was drawn between time (Jan-Sep) and % snow covered area (SCA).

The snow depletion curves of years 2005 and 2006 show that zone first and second snow was almost melted in April–May respectively. In 2005, snow of zone third and fourth was completely melted in June and July respectively. In 2006, snow of third zone completely melted in July and zone fourth in August.

The snow depletion curves of year 2007 and 2008 show that in first and second zone snow was almost melted in April as. In 2007, zone third and fourth snow was completely melted in May and June respectively. In 2008, zone third and fourth snow completely melted in May and June respectively. The snow melting period is increasing while snow accumulation period is decreasing due to increasing temperature in UIB.

The depletion of snow covered area during years 2009 and 2010 show that zone first and second snow was almost melted in April. In 2009, zone third snow completely melted in July while in zone fourth snow was completely melted in September. In 2010, zone third and fourth snow was completely melted in July and September respectively. The zone 5 and 6, snow did not completely melt because these zones are above 4400m elevation and there is permanent snow on it.

The snow depletion photographs for the year 2001 indicate that the process of snow depletion begins in April in lower elevation areas and gradually progresses to higher elevation areas. The elevated regions of Gilgit are characterized by the presence of glaciers. The process of glacier melting commences in July following the thawing of seasonal snow. The process of glacier melting is gradual and does not reach completion until the accumulation period begins in October, as depicted in Fig. 15.

Snowmelt Runoff Model

Calibration of SRM Model

The Snowmelt Runoff Model (SRM) was calibrated against four years 2001 to 2004.The input data of variable and parameter was used. Calibrated parameter are shown Table 15.

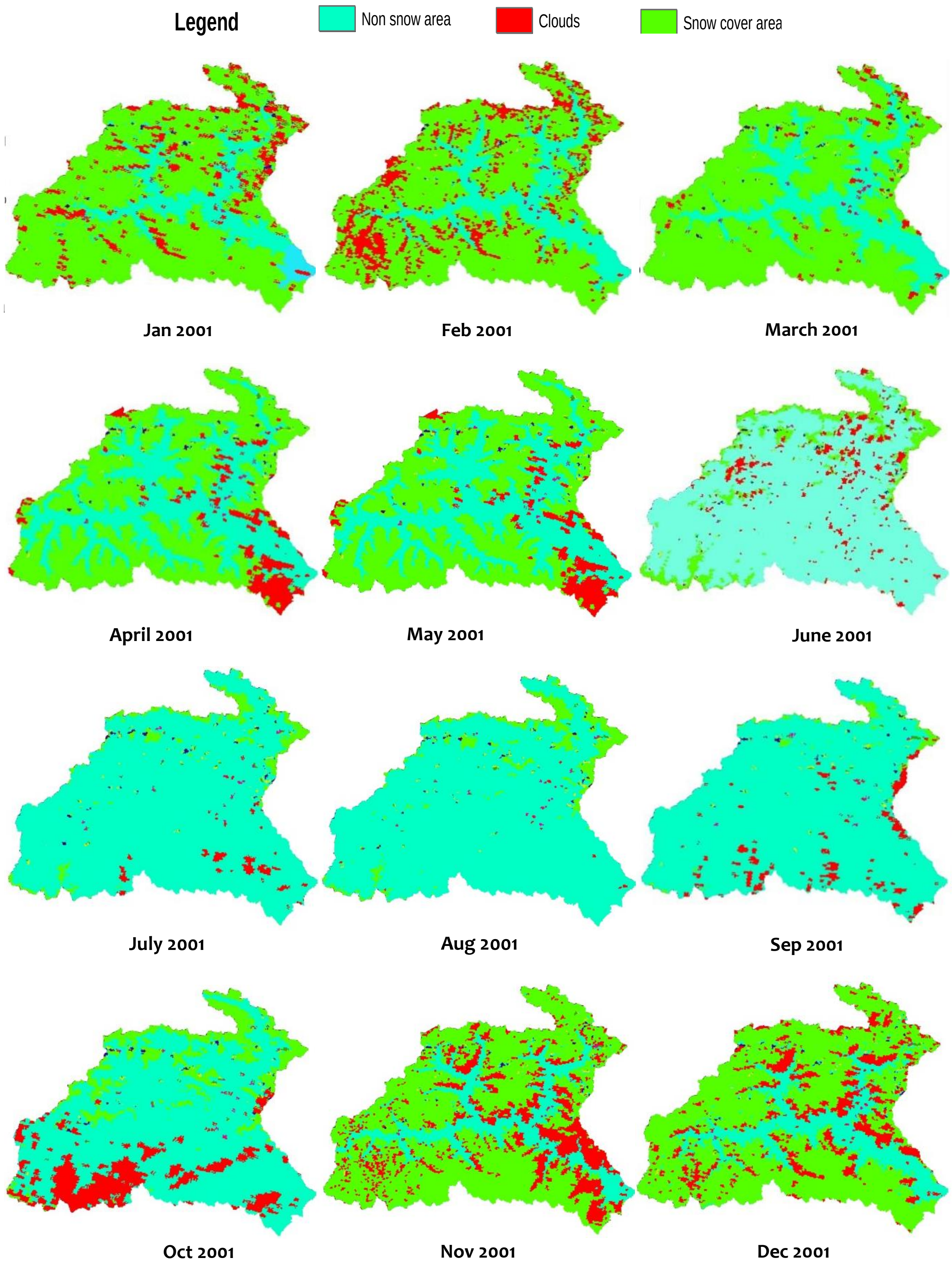

Fig. 15: Snow Depletion Image of Gilgit of 2001 in Different Months.

The temperature lapse rate for the Gilgit River basin was determined to be 0.64 °C/100m. This calculation was based on the temperature difference observed between the climate stations located at the lowest elevation (Gilgit) and the highest elevation (Ushkor). The sensitivity of this number is crucial as it directly influences the extrapolation of base station temperature to high altitude. The critical temperature determines whether the observed or predicted precipitation will be in the form of snow or rain. It is especially crucial during the snow accumulation phase, as opposed to the ablation period. Accurate long-term temperature data, including snow and rainfall records, are necessary to estimate essential temperature levels. If the temperature is below the critical temperature (Tcrit), there is a possibility of snowfall. Gilgit is situated in a glaciated area. At high altitudes above (3000m) the winter average temperature reached -8 to -10°C and most precipitation in the form of snow occurred over 3000 meters in elevation. On the base of the observed data value of critical temperature was used at 0°C. The rainfall threshold was used 6.0 cm in the model which is the default value. The degree day factor ‘a’ converts the number of degree day values T [°C.d] into daily snowmelt depth M [cm].

M=a×T

In the absence of detailed data value of degree day factor can be found by using empirical formula (Martinec, 1996):

$a = 1.1\ \rho s/\rho w$

a = degree day factor [cm°C^{-1}d^{-1}]

ρw = density of water

ρs= density of snow

The degree day value is not constant; it fluctuates in accordance with the changing snow qualities during the snowmelt season. The value of the snow increases as it ages due to a decrease in its albedo. The degree day factor for the area can be calculated if the snow density data is accessible, as it serves as a reliable predictor of albedo (Rango and Martinec, 1995). In glaciated basins, the degree-day factor typically surpasses 0.6 cm C-1d-1 by the end of summer, when the ice becomes visible (Kotlyakov and Krenke, 1982). Given that Gilgit is a glaciated basin, a value of 0.3 was utilized at the beginning of the snowmelt season, while a value of 0.75 was employed towards the end of the snowmelt season. The range of values used in SRM is between 0.3 and 0.75 cm°C-1d-1.

The disparity between the total water volume (comprising both snow and rainfall) and the outflow from the basin is attributed to many factors such as infiltration, evaporation, and evapotranspiration. The runoff coefficients for rainfall (CR) and snow (CS) consider these losses. These measures quantify the proportion of snow and rainfall that is transformed into runoff. The estimation of these parameters was derived from extensive records of precipitation and runoff over an extended period of time. The daily precipitation data over an extended period was collected and then multiplied by the whole area of the basin. The runoff volume was determined and subsequently divided by the daily discharge at the basin outlet to produce the runoff coefficient. The CR and CS values utilized in the SRM vary between 0.05 and 0.45 for rain and between 0.03 and 0.48 for snow, respectively, during the snow melt period. The highest level of fitness was seen between the measured and calculated discharge during the calibration period, in relation to these values. The rainfall contributing area (RCA) value was set to 0 in the model from October to April. This is because during these months, the rainfall is trapped by snow and freezing conditions, and only converted to runoff in areas without snow. During the snowmelt phase, the RCA value was set to 1. This is because when snow is mature and rain falls on it, it is expected that an equal quantity of water is released from the snowpack, resulting in increased runoff (rain + snow).

The recession coefficient is a crucial characteristic of the Soil Retention Model (SRM), and (1-k) represents the proportion of daily meltwater that directly contributes to the runoff. Recession coefficients quantify the proportion of the discharge that comes from snowmelt from the previous day on a specific day. Examining historical discharge data is typically an effective method for determining the value of k. The method to locate it involves graphing long-term historical discharge data on a log-log scale and calculating the recession coefficient daily, which corresponds to the slope of the best-fit line. The value of K is not constant but varies proportionally with the decreasing Q, as described by the equation below:

$K_{n+1} = x \times Q_n^{-y}$

The value of recession coefficients used in the model was Xcoeff. =1.08-1.09 and Ycoeff. =0.02. The default value of lag time used in the model was used which is 18 hrs.

Calibration of SRM for Gilgit River Basin

The Snowmelt Runoff Model (SRM) was calibrated for Gilgit River Basin. The flow data of Gilgit stream gauging station was used. The climatic data of high altitude station Ushkore and Yasin and low elevation station Gilgit was used .The average of temperature and precipitation of these three stations was used as input in Snowmelt Runoff Model. The model simulation was compared with the observed discharge for four years 2001 to 2004.

Validation of SRM

The SRM after calibration was validated on years 2005 and 2006.

Year Round Simulation of SRM

The SRM model after calibration and validation was applied on Gilgit catchment for the year 2008 to 2010.The results show that model performance is good.

Contribution of Snow and Rainfall (%) to Total Runoff of Gilgit River

The above Fig. 16 showed the percentage of daily snowmelt, rainfall depth and melted precipitation in the form of snow in the cumulative runoff of Gilgit river catchment for the year 2006.

The Table 6 shows in Gilgit River basin contribution of initial snow is more that is about 78.3% as compared to rainfall whose contribution is 19.5% while contribution of new snow to runoff is less and it is about 2.2%.

Climate Change Modeling using SRM

The SRM was utilized to simulate forthcoming fluid dynamics. Climate change scenarios were generated in the context of SRM (Solar Radiation Management). The future forecasts produced by the PRECIS model were utilized in the SRM for the prediction of forthcoming flows. The data was obtained from the "Numerical Modeling group of the Research and Development Division, Pakistan Meteorological Department (PMD), Islamabad, Pakistan" to conduct Regional Climate Model simulations.

Impact of Avg. Annual Temperature

Recently Pakistan Meteorological Sub-Department, Research and Development Division (R&D) used ECHAM5 data for the A1B scenario and downscaled it with the PRECIS

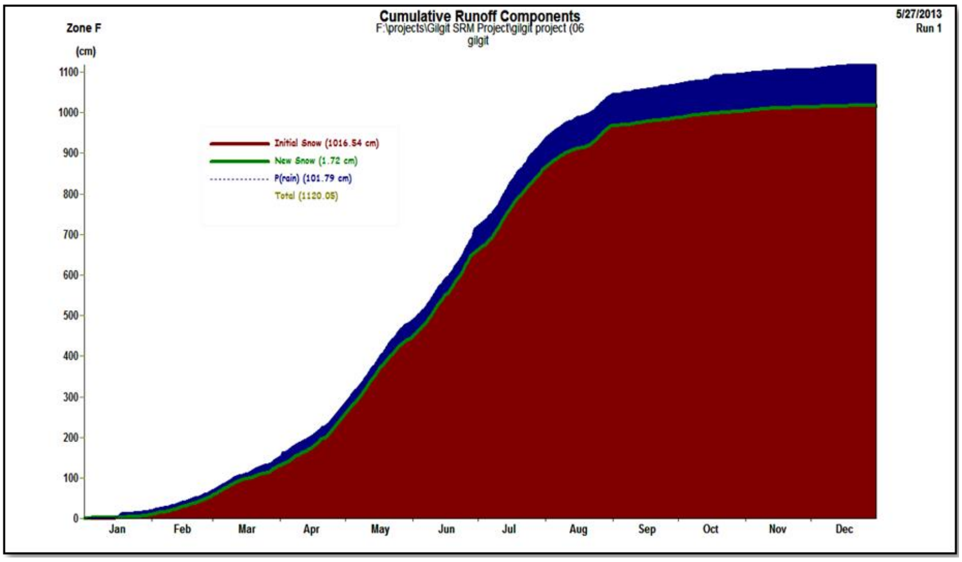

Fig. 16: Cumulative runoff components of Gilgit River for the year 2006

Regional Climate Model. The baseline period used was 1961-1990. The future projections were made from 2011-2100. The resolution of the model was used 25km and 50km. The model was applied all over Pakistan including Gilgit Catchment. The scenarios of precipitation, maximum, minimum, and mean temperature were used in the Snowmelt Runoff Model (SRM) and future flows of the Gilgit River were predicted. The climate scenario A1 is based upon that economic growth per capita will increase, the population will increase till 2050 and then decline and there will be strong regional interactions and income convergence. On this base, the model developed future trends of temperature and precipitation. According to this scenario, A1B, Gilgit catchment mean annual temperature would increase about 0.30°C from (2011 to 2030), 1.30°C from (2031 to 2050) and 3.1°C from (2051 to 2099). The overall increase in mean annual temperature of the Gilgit catchment will be 4.7°C at the end of the 21st century. These scenarios were used in SRM for the prediction of future flows of the Gilgit River.

Impact of fall in Average Annual Temperature

The summer flows will decrease by 3% due to decrease in average annual temperature by 1°C and the summer flows will decrease by 7% due to decrease in average annual temperature by 2°C as shown in Table 7.

Future Scenarios of Max/Min. Temperature

The future climate change scenarios of Gilgit developed through the regional climate model (PRECIS_25km resolution) by using the A1B emission scenario. The future data generated by the regional climate model showed an increasing trend in both maximum and minimum temperatures from (2011 to 2099). The results show that the increase in winter maximum temperature is greater as compared to summer and annual maximum temperature. It shows that there is an increasing trend in annual and summer minimum temperatures while in winter minimum temperatures there is decreasing trend. The results obtained from Mann-Kendall trend test are given below:

Impact of rise in Max/ Min. Temperature

The data presented in Tables 10 and 11 indicate a consistent upward trend in both the maximum and minimum winter temperatures in Gilgit from 2011 to 2099. The snowmelt runoff model utilized the mean winter maximum and lowest temperatures to forecast the future flows of the Gilgit River, as outlined in Table 12.

The Table 12 shows that by increasing annual maximum and minimum temperature to 1.24°C, summer flows will increase by 16% and when this temperature is increased to 2.78°C, summer flows will increase by 34%.

In all the hydrographs blue line shows observed runoff while red line shows increase in runoff due change in climatic parameter temperature. Due to rise in temperature, seasonal snow and glacier melt due which flows in rivers increase.

Impact of rise in Winter Max/ Min. Temperature

The data presented in Table 11 indicates a projected increase in both the maximum and minimum winter temperatures in Gilgit from 2011 to 2099.The snowmelt runoff model utilized the mean winter maximum and lowest temperatures to forecast the future flows of Gilgit River, as outlined in Table 11.

Table 11 shows that there is a slight increase in winter maximum, and minimum temperatures till 2030 and there will be a rapid increase in winter maximum, and minimum temperatures after 2050 in Gilgit.

Impact of Rise in Summer Max/ Min. Temperature

The summer maximum and minimum temperatures in Gilgit exhibit an upward trend from 2011 to 2050, followed by a downward trend from 2051 to 2099. The snowmelt runoff model utilized the mean summer maximum and minimum temperatures to forecast the future flows of the Gilgit River, as outlined in Table 12.

Table 12 shows that due to this increase in temperature summer flows in Gilgit River will increase by 12% till 2030 and 16% till 2050.No significant change in summer temperature was observed after 2050.

Impact of Increase in Cryosphere Area

The findings from the Regional Climate Model (PRECIS_25 km) indicate a notable rise in winter precipitation within the Gilgit River basin, with further increases projected for the future. Based on this rise, scenarios were built to assess the potential effects of a 10% to 20% increase in cryosphere area in Gilgit due to increased winter precipitation. The question is: what impact will this have on future flows? These scenarios were employed in SRM and it was noted that augmenting the cryosphere area to 10% resulted in a 13% rise in summer flows, while increasing the cryosphere area to 20% led to a 27% increase in summer flows in the Gilgit River.

Conclusion

The following specific conclusions have drawn from the results of this study:

1. The overall mean basin maximum temperature is 10 ºC and varies from -2.5ºC to 23.4ºC while the minimum temperature is 1.2ºC and varies from -8.3ºC to 12.2ºC. Mean annual precipitation ranges from around 148 mm to 700 mm with mean basin precipitation is 350 mm.
2. The mean monthly flow of the basin is 288 cusec. The water yield of the basin is found to 9.09 BCM (750 mm)
3. Gilgit River basin contribution of initial snow is more that is about 78.3% as compared to rainfall whose contribution is 19.5% while contribution of new snow to runoff is less and it is about 2.2%.
4. Mean annual temperature would increase about 0.30°C from (2011 to 2030), 1.30°C from (2031 to 2050) and 3.1°C from (2051 to 2099).The overall increase in mean annual temperature of Gilgit catchment will be 4.7°C at the end of 21st century.
5. By increasing annual maximum and minimum temperature to 1.24°C, summer flows will increase by 16% and when this temperature is increased to 2.78°C, summer flows will increase by 34%.
6. It was observed that if cryosphere area is increased to 10%, summer flows will increase by 13% and if cryosphere area is increased to 20%, summer flows will increase by 27% in Gilgit River
7. The contribution of snow + glacier melt is 78.3, new snow is 2.2, rain is 19.5 of total runoff of Gilgit River

Recommendations

1. To manage the Gilgit watershed its physical characterization and monitoring system must be implemented for all aspects of watershed health, i.e current hydrological processes, glacier melting processes and river morphology to understand the dynamics of changing climate.
2. The places that are prone to disasters must be clearly identify and activities like Streams and channels must be kept clear from any sort of hurdle that may lead to flood or flash flood at the downstream and mitigation plans must be implemented at the study area in case of any natural disaster.
3. There should be higher temporal resolution of satellite imagery.
4. There should be joint cooperation with ministries like Ministry of Water, Agriculture, Nature Protection and Emergency Situation etc.
5. Gauged stations must be developed to measure the flows of River Gilgit and its tributaries so that discharge could be calculated for utilization in insitu power generation activities.
6. The climatic stations within the Gilgit River basin may be used to study the behaviour of stream movement at Dainyor Bridge in the future.

It is necessary to replicate this study in the same and other basins for multiple years in order to obtain a comprehensive understanding of the inputs and outputs. This approach can then be utilized to anticipate runoff during the melting season in Northern Pakistan.

REFERENCES

Adam, J. C., Hamlet, A. F., & Lettenmaier, D. P. (2009). Implications of global climate change for snowmelt hydrology in the twenty-first century. *Hydrological Processes*, *23*(7), 962-972.

Ahmad, Z., Hafeez, M., & Ahmad, I. (2012). Hydrology of mountainous areas in the upper Indus Basin, Northern Pakistan with the perspective of climate change. *Environmental Monitoring and Assessment*, *184*(9), 5255-5274.

Archer, D. R., & Fowler, H. J. (2004). Spatial and temporal variations in precipitation in the Upper Indus Basin, global teleconnections and hydrological implications. *Hydrology and Earth System Sciences Discussions*, *8*(1), 47-61.

Baede, A. P. M., Ahlonsou, E., Ding, Y., & Schimel, D. S. (2001). The climate system: an overview. In J.J. Maccarthy, O. F. Canziani, & N. A. Leary (Eds.), *Climate Change 2001: impacts, adaptation and vulnerability* (pp. 87-98). New York: Cambridge University Press.

Bajracharya, S. R., & Shrestha, B. R. (2011). *The status of glaciers in the Hindu Kush-Himalayan region*. International Centre for Integrated Mountain Development (ICIMOD).

Bolch, T. (2007). Climate change and glacier retreat in northern Tien Shan (Kazakhstan/Kyrgyzstan) using remote sensing data. *Global and Planetary Change*, *56*(1-2), 1-12.

Bookhagen, B., & Burbank, D. W. (2010). Toward a complete Himalayan hydrological budget: Spatiotemporal distribution of snowmelt and rainfall and their impact on river discharge. *Journal of Geophysical Research: Earth Surface*, *115*(F3).

Dhami, B., Himanshu, S. K., Pandey, A., & Gautam, A. K. (2018). Evaluation of the SWAT model for water balance study of a mountainous snowfed river basin of Nepal. *Environmental Earth Sciences*, *77*, 1-20.

Farhan, M., Yang, J., Wu, T., Wang, S., Zhao, X., & Tariq, A. (2024). Impact assessment of agricultural droughts on water use efficiency in different climatic regions of Punjab Province Pakistan using MODIS time series imagery. *Hydrological Processes*, *38*(7), e15232.

Fowler, H. J., & Archer, D. R. (2006). Conflicting signals of climatic change in the Upper Indus Basin. *Journal of Climate*, *19*(17), 4276-4293.

Immerzeel, W. W., Pellicciotti, F., & Bierkens, M. F. P. (2013). Rising river flows throughout the twenty-first century in two Himalayan glacierized watersheds. *Nature Geoscience*, 6(9), 742.

Immerzeel, W. W., Van Beek, L. P. H., Konz, M., Shrestha, A. B., & Bierkens, M. F. P. (2012). Hydrological response to climate change in a glacierized catchment in the Himalayas. *Climatic Change*, *110*(3-4), 721-736.

Khan, N., & Shahid, S. (2024). Urban heat island effect and its drivers in large cities of Pakistan. *Theoretical and Applied Climatology*, *155*(6), 5433-5452.

KOTLYAKOV, V., & KRENKE, A. (1982). Institut Geografii, Akademiya Nauk SSSR, Moscow, USSR ABSTRACT Hydrological conditions of the alpine zone are hard to reveal because of the difficulty of organizing. *Hydrological Aspects of Alpine and High-mountain Areas*, (2723), 31.

Liang, S., Fang, H., Chen, M., Shuey, C. J., Walthall, C., Daughtry, C., ... & Strahler, A. (2002). Validating MODIS land surface reflectance and albedo products: Methods and preliminary results. *Remote sensing of environment*, *83*(1-2), 149-162.

Lightfoot, H. D., & Ratzer, G. (2024). Reliable Physics Demand Revision of the IPCC Global Warming Potentials. *Journal of Basic & Applied Sciences*, *20*, 54-58.

Martinec, Z. (1996). Stability investigations of a discrete downward continuation problem for geoid determination in the Canadian Rocky Mountains. *Journal of Geodesy*, *70*(11), 805-828.

Pomeroy, J. W., & Brun, E. (2001). Physical properties of snow. *Snow ecology: An interdisciplinary examination of snow-covered ecosystems*, *45*, 118.

Rango, A., & Martinec, J. (1995). Revisiting the degree-day method for snowmelt computations. *JAWRA Journal of the American Water Resources Association*, *31*(4), 657-669.

Rango, A., & MARTINEC, J. C. (2008, September). Predictions for snow cover, glaciers and runoff in a changing climate. In *Hydrology and Water Resources International Conference Proceedings* (pp. 277-280).

Schumm, S. A. (1956). Evolution of drainage systems and slopes in badlands at Perth Amboy, New Jersey. *Geological society of America bulletin*, *67*(5), 597-646.

Strahler, A. N. (1964). Quantitative geomorphology of drainage basin and channel networks. *Handbook of applied hydrology*.

Sirguey, P., Mathieu, R. & Arnaud, Y. (2009). Subpixel monitoring of the seasonal snow cover with MODIS at 250m spatial resolution in the Southern Alps of New Zealand: Methodology and accuracy assessment. *Remote Sensing of Environment*, *113*(1), 160-181.

Tanmoyee, B., & Abdul, R. P. H. (2015). Climate Change Impact on Snowmelt Runoff Modelling for Alaknanda River Basin. *Methodology*, 5(11).

Zhang, X., Srinivasan, R., Debele, B., & Hao, F. (2008). Runoff simulation of the headwaters of the yellow river using The SWAT model with three snowmelt algorithms 1. *JAWRA Journal of the American Water Resources Association*, *44*(1), 48-61.